Efficient DMFT-simulation of the Holstein-Hubbard Model

Philipp Werner and Andrew J. Millis
Columbia University, 538 West, 120th Street, New York, NY 10027, USA
(Dated: August 16, 2007)

We present a method for solving impurity models with electron-phonon coupling, which treats the phonons efficiently and without approximations. The algorithm is applied to the Holstein-Hubbard model in the dynamical mean field approximation, where it allows access to strong interactions, very low temperatures and arbitrary fillings. We show that a renormalized Migdal-Eliashberg theory provides a reasonlable description of the phonon contribution to the electronic self energy in strongly doped systems, but fails if the quasiparticle energy becomes of order of the phonon frequency.

PACS numbers: 71.10.Fd, 71.28.+d, 71.30.+h, 71.38.k

Electron-lattice interactions play a fundamental role in the physics of metals. In conventional ("weakly correlated") materials such as Al or MgB_2, phonons are the dominant source of inelastic scattering and provide the pair binding which leads to superconductivity. In these materials, physical understanding is greatly aided by the Migdal-Eliashberg theory, which justifies the use of density functional band theory methods to estimate the electron-phonon coupling constants and perturbative methods to estimate electron mass renormalizations, lifetimes and pairing strengths. A key result of the Migdal-Eliashberg theory is that the effect of the electrons on the phonons is a renormalization of the phonon oscillator frequency ω_0, while the effect of the phonons on the electrons is an increase in the electron effective mass. The mass increase "turns on" at frequencies below the renormalized phonon frequency.

In unconventional ("strongly correlated") materials such as the high temperature superconductors [1], the fullerenes [2, 3], or the colossal magnetoresistance rare-earth manganites [4, 5] the situation is less clear. Many experiments suggest that electron-phonon effects are important. For example, in high T_c superconductors changes attributed to the electron-phonon coupling are observed in the electronic dispersion [1] at energies of the order of typical optical phonon frequencies. However, there is as yet no clear theoretical basis for interpreting these or related data in strongly correlated materials. While there has been extensive and important work on static properties of models involving electron-electron and electron-phonon coupling [6, 7], on Fermi-liquid and effective field theory based approaches [8, 9], on the Holstein model [10] and on the (bi-)polaron problem (one or two interacting electrons) [11, 12] less is known about the dynamical consequences of the electron-phonon interaction in strongly correlated materials.

A way forward is provided by dynamical mean field theory (DMFT), a powerful, non-perturbative tool to study the properties of strongly correlated systems, which has provided considerable insight into the correlation induced metal-insulator (Mott) transition [13]. Progress in using dynamical mean field methods to study phonons coupled to strongly correlated electrons [14, 15, 16] has been hampered by the mismatch in energy scales between the electronic and lattice parts of the problem and by the difficulty of providing a quantitative treatment of the low temperature properties of strongly correlated materials even in the absence of electron-phonon coupling. In this paper we introduce a new method which resolves these problems and allows the DMFT simulation of important classes of models at essentially the same computational expense as the corresponding models without coupling to phonons.

We consider the Holstein-Hubbard Hamiltonian

$$\begin{aligned} H &= -\sum_{i,\delta,\sigma} t(\delta) c^\dagger_{i+\delta,\sigma} c_{i,\sigma} + \sum_i [U n_{i,\uparrow} n_{i,\downarrow} - \mu(n_{i,\uparrow}+n_{i,\downarrow})] \\ &\quad +\lambda \sum_i (b^\dagger_i + b_i)(n_{i,\uparrow}+n_{i,\downarrow}-1) + \omega_0 \sum_i b^\dagger_i b_i, \end{aligned} \tag{1}$$

where U denotes the on-site repulsion, μ the chemical potential of the electrons with creation operators $c^\dagger_\sigma$ and density operators n_σ, $b^\dagger$ the creation operator for Einstein phonons of frequency ω_0, and the electron-phonon coupling is λ.

The single-site DMFT approximation [13] reduces the problem to the self-consistent solution of a quantum impurity model specified by the Hamiltonian $H_{\rm QI} = H_{\rm loc} + H_{\rm hyb} + H_{\rm bath}$. Here, the local term is

$$\begin{aligned} H_{\rm loc} &= -\mu(n_\uparrow + n_\downarrow) + U n_\uparrow n_\downarrow \\ &\quad +\lambda(n_\uparrow + n_\downarrow - 1)(b^\dagger + b) + \omega_0 b^\dagger b, \end{aligned} \tag{2}$$

and the impurity-bath mixing and bath Hamiltonians are $H_{\rm hyb} = \sum_{p,\sigma}(V_{p,\sigma} c^\dagger_\sigma a_{p,\sigma} + V^*_{p,\sigma} c_\sigma a^\dagger_{p,\sigma})$ and $H_{\rm bath} = \sum_{p,\sigma} \epsilon_p a^\dagger_{p,\sigma} a_{p,\sigma}$. The parameters $V_{p,\sigma}$ and ϵ_p are determined by a self-consistency equation.

In the absence of electron-phonon coupling, $H_{\rm loc}$ has a small Hilbert space and one energy scale (U). Adding an electron-phonon coupling introduces a new energy scale, the phonon frequency ω_0, and requires keeping track of the bosonic sector of the Hilbert space (with an infinite number of states). Previous approaches to the problem have involved either treating the bosons semiclassically [14, 17] or truncating the boson Hilbert space, retaining

only a finite number of boson states [15, 16]. The semi-classical approach cannot account for quantal phonon effects such as electronic mass renormalization or superconductivity, while treating even a truncated boson Hilbert space directly is computationally expensive.

In Refs. [18, 19] we have shown that the stochastic sampling of a diagrammatic expansion of the partition function in powers of the impurity-bath hybridization term $H_{\rm hyb}$ leads to a highly efficient [20] impurity solver for purely electronic models. After tracing out the bath states $a_{p,\sigma}$, the weight of a Monte Carlo configuration corresponding to a perturbation order n (n creation operators $c^\dagger_\sigma(\tau_\sigma)$ and n annihilation operators $c_\sigma(\tau'_\sigma)$) can be expressed as

$$w(\{O_i(\tau_i)\}) = Tr_c\Big\langle T_\tau e^{-\int_0^\beta d\tau H_{\rm loc}(\tau)} O_{2n}(\tau_{2n})\dots \\ \dots O_2(\tau_2)O_1(\tau_1)\Big\rangle_b d\tau_1\dots d\tau_{2n}\prod_\sigma(\det M^{-1}_\sigma)s_\sigma, \quad (3)$$

with $O_i(\tau_i)$ the (time ordered) creation and annihilation operators for spin up or down electrons on the impurity site. The matrix elements $(M^{-1}_\sigma)_{i,j} = F_\sigma(\tau'_{\sigma,i} - \tau_{\sigma,j})$ are determined by the $V_{p,\sigma}$ and ϵ_p through the hybridization functions $F_\sigma(-i\omega_n) = \sum_p \frac{|V_{p,\sigma}|^2}{i\omega_n - \epsilon_p}$ [19]. The sign s_σ is 1 if the σ-spin operator with the lowest time argument is a creation operator and -1 otherwise.

To evaluate $\langle\cdots\rangle_b$ we use a Lang-Firsov [21] transformation. Defining operators $X = (b^\dagger + b)/\sqrt{2}$ and $P = (b^\dagger - b)/i\sqrt{2}$, the unitary transformation specified by e^{iPX_0} shifts X by $X_0 = (\sqrt{2}\lambda/\omega_0)(n_\uparrow + n_\downarrow - 1)$ so that

$$\begin{aligned}\tilde{H}_{\rm loc} &= e^{iPX_0}H_{\rm loc}e^{-iPX_0} \\ &= -\tilde{\mu}(\tilde{n}_\uparrow + \tilde{n}_\downarrow) + \tilde{U}\tilde{n}_\uparrow\tilde{n}_\downarrow + \frac{\omega_0}{2}(X^2 + P^2) \quad (4)\end{aligned}$$

has no explicit electron-phonon coupling. $\tilde{H}_{\rm loc}$ is of the Hubbard form but with modified chemical potential and interaction strength: $\tilde{\mu} = \mu - \lambda^2/\omega_0$, $\tilde{U} = U - 2\lambda^2/\omega_0$. Also, the electron creation and annihilation operators are transformed according to $\tilde{c}^\dagger_\sigma = e^{\frac{\lambda}{\omega_0}(b^\dagger - b)}c^\dagger_\sigma$ and $\tilde{c}_\sigma = e^{-\frac{\lambda}{\omega_0}(b^\dagger - b)}c_\sigma$. The phonon contribution w_b to the weight (3) is $w_b(\{O_i(\tau_i)\}) = \left\langle e^{s_{2n}A(\tau_{2n})}\cdots e^{s_1A(\tau_1)}\right\rangle_b$ with $0 \le \tau_1 < \ldots < \tau_{2n} < \beta$, $s_i = 1$ (-1) if the $n^{\rm th}$ operator is a creation (annihilation) operator and $A(\tau) = \frac{\lambda}{\omega_0}(e^{\omega_0\tau}b^\dagger - e^{-\omega_0\tau}b)$. This expectation value, taken in the thermal state of free bosons, evaluates to

$$w_b(\{O_i(\tau_i)\}) = \exp\Bigg[-\frac{\lambda^2/\omega_0^2}{e^{\beta\omega_0}-1}\Big(n\big(e^{\beta\omega_0}+1\big) \\ + \sum_{2n\ge i>j\ge 1} s_i s_j\big\{e^{\omega_0(\beta-(\tau_i-\tau_j))} + e^{\omega_0(\tau_i-\tau_j)}\big\}\Big)\Bigg], \quad (5)$$

and the weight (3) becomes the product

$$w(\{O_i(\tau_i)\}) = w_b(\{O_i(\tau_i)\})\tilde{w}_{\rm Hubbard}(\{O_i(\tau_i)\}), \quad (6)$$

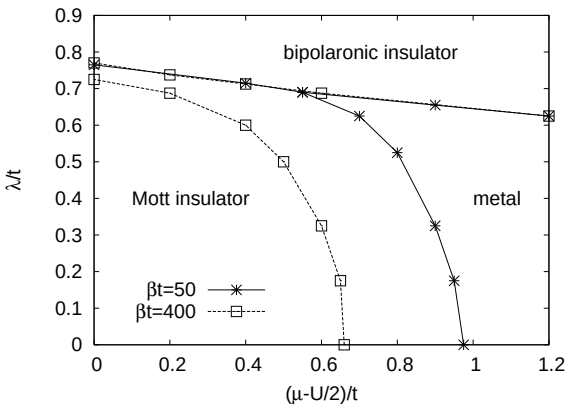

FIG. 1: Phase diagram for $\omega_0 = 0.2t$, $\beta t = 50, 400$ and $U/t = 6$ in the plane of chemical potential μ and phonon coupling strength λ. Half-filling corresponds to $\mu = U/2$. In the metallic phase, the filling increases with increasing μ, λ.

where $\tilde{w}_{\rm Hubbard}$ is the weight of a corresponding configuration in the Hubbard impurity model (without phonons, but modified parameters $\tilde{U}$ and $\tilde{\mu}$). The Holstein-Hubbard model can thus be simulated without truncation at an expense comparable to the Hubbard model. Superconducting phases can be simulated in the same way, using the formalism outlined in Ref. [13]; the only difference is that the determinant in Eq. (3) can no longer be factorized into spin components.

We have applied our method to the Holstein-Hubbard model with a semi-circular density of states of bandwidth $4t$ and $\omega_0/t = 0.2$. For reasons of space, we restrict our attention to non-superconducting phases. Figure 1 shows the phase diagram at $U/t = 6$ in the space of chemical potential and phonon coupling. Our results at half-filling are in good agreement with those computed by NRG [15]. If the chemical potential is increased at fixed electron-phonon coupling, a transition to a metal occurs. The shift in critical μ with temperature arises from the entropic stabilization of the insulating phase and is roughly λ-independent. The transition is first order at $T > 0$ (with a jump in density), but apparently becomes continuous as $T \to 0$. The critical chemical potential decreases as the electron-phonon coupling is increased. This behavior is physically expected: increasing the phonon coupling reduces the effective interaction $\tilde{U}$ and so the magnitude of the insulating gap. We have confirmed this by analysis of the Green function. Our finding appears to contradict Ref. [16] which stated that the electron-phonon coupling stabilizes the insulating state. The apparent difference arises from a choice of convention: the authors of Ref. [16] couple the phonons to the total density n, which implies a λ-dependent shift in chemical potential which was interpreted as a physical stabilization. We couple the phonons to the difference in density from the half filled value, which eliminates this

(physically irrelevant) shift at half filling.

We now turn to the frequency dependence of the electron self energy. In weakly correlated materials the conduction-band electrons renormalize the phonon propagator D from its bare value D_0 according to the RPA (ladder) result $D^{-1} = D_0^{-1} - \lambda^2\chi_0$ with χ_0 the bare (no phonons) electronic density-density correlator. The Migdal-Eliashberg approximation also implies that the local density-density correlator χ is given by

$$\chi(\Omega) = \chi_0(\Omega)/(1 - \lambda^2 D_0(\Omega)\chi_0(|\Omega|)). \qquad (7)$$

The electron self energy is given in frequency space by the convolution $\Sigma = \lambda^2 G_0 * D$. It is convenient to present results as the Matsubara axis mass renormalization factor $r(i\omega_n) = -\Im m\Sigma(i\omega_n)/\omega_n$. According to Migdal-Eliashberg theory, the effect of the electron-phonon coupling is to add to the purely electronic $r(i\omega_n)$ a term approximately of the form

$$r_{ME}(i\omega_n) = (2\lambda^2 N_0/\omega_n)\arctan(\omega_n/\omega_0^{\rm ren}) \qquad (8)$$

with N_0 the Fermi surface density of states (in our case $\approx 1/2\pi t$). The zero frequency limit gives the electron-phonon contribution to the Fermi surface mass enhancement $m^*_{ME}/m = \frac{2\lambda^2 N_0}{\omega_0^{\rm ren}}$ and r_{ME} drops to about half of its zero frequency value around $2\omega_0^{\rm ren}$.

The upper panel of Fig. 2 compares the density-density correlation function computed from Eq. (7) to $\chi(\tau)$ measured in our QMC simulations, for $U = 0$ and several values of λ. Good agreement is seen; the small shift of λ required to match the $\lambda = 0.3$ QMC data ($\lambda_{\rm eff} \approx 0.275$) is a beyond-Migdal effect arising from the small but non-vanishing effect of the electron self energy on χ_0. $\chi(\tau)$ increases with λ because density fluctuations can transform into phonons. The intermediate-time exponential decay visible in the figure gives the renormalized phonon frequency $\omega_0^{\rm ren}$, while in the regimes where there is no clear evidence of exponential decay the phonon frequency is not significantly renormalized. For $U > 0$ the computed $\chi(\tau)$, shown in the lower panel of Fig. 2, also exhibits an exponential decay, from which we estimate $\omega_0^{\rm ren}$.

Figure 3 presents the phonon-induced change in the mass renormalization function $\Delta r = -\Im m\left(\Sigma(\lambda,\delta,\omega_n) - \Sigma(0,\delta,\omega_n)\right)/\omega_n$. The upper panel shows results for $U = 4t$, less than the Mott critical value $U_{c2} \approx 5.8t$. At half filling (curves traced out by symbols) we find, in agreement with Ref. [15], that the phonon contribution to the mass enhancement has the "wrong" sign, except for couplings very close to the bipolaronic instability: the dominant effect of the phonons is the reduction of U. A new result is that (again except for the largest λ) there is no obvious feature at the renormalized phonon frequency. The blue lines present the doping dependence at fixed $\lambda = 0.4t$. We see that as the doping is increased, a result compatible with Migdal-Eliashberg theory is eventually recovered. The lower panel shows

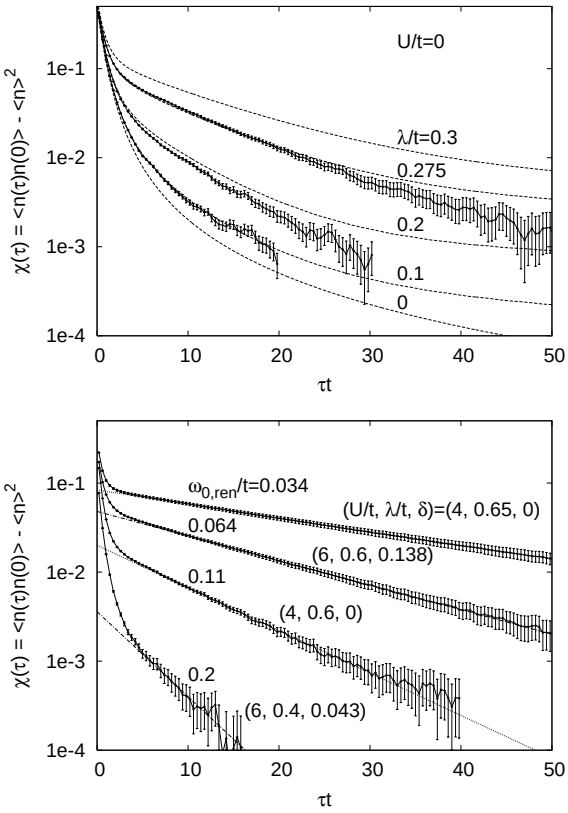

FIG. 2: Imaginary time dependence of the density-density correlation function plotted on a log-scale to highlight the intermediate time exponential decay. If no exponential regime is visible, the phonon frequency is not renormalized; otherwise $\omega_0^{\rm ren}$ can be extracted from the slope. Upper panel: $U = 0$ and $n = 1$. Dashed lines: $\chi(\tau)$ from Eq. (7) for indicated phonon couplings. Solid lines with 1-σ error bars show the QMC results for $\beta t = 400$ and $\lambda/t = 0.1$, 0.2, 0.3 (from bottom to top). Lower panel: correlation functions for the interacting model at half filling, $U/t = 4$ and $\lambda/t = 0.6$, 0.65 and in the doped Mott insulator at $U/t = 6$, $\lambda/t = 0.4$, 0.6 (dopings per spin $\delta = 0.043$, 0.138).

the behavior for $U = 6t$, greater than the Mott critical value. Here we find again that for moderate electron phonon couplings and relatively highly doped samples, a renormalized Migdal-Eliashberg theory (with perhaps a slightly reduced effective electron phonon coupling $\lambda_{\rm eff}$) provides a reasonably consistent description of the data, except that Δr drops more rapidly for $\omega_n \gg \omega_0$. However, when the quasiparticle energy $E_F/(1-\partial\Sigma/\partial\omega)$ becomes of order of the phonon frequency (as happens at $\delta = 0.04$) or the coupling approaches the bipolaronic instability ($\lambda = 0.6t$) the Migdal-Eliashberg description breaks down. For large λ, $r_{ME}(i\omega_n)$ drops too rapidly, while near the doping driven Mott transition, the shape is too broad. Nevertheless, unlike in the half-filled metal shown in the upper panel of Fig. 3, in the weakly doped Mott insulator, the upturn in the mass renormalization

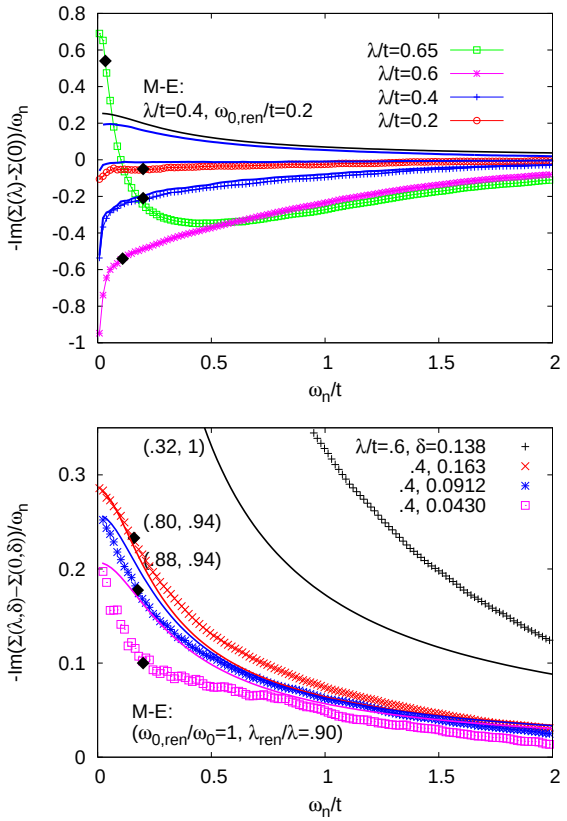

FIG. 3: (Color online) Phonon contribution to the electronic self energy at $\beta t = 400$. Black diamonds: renormalized phonon frequency $\omega_0^{\rm ren}$. Upper panel: $U/t = 4$. Symbols: half filling, λ values indicated. Blue lines: $\lambda/t = 0.4$ and doping per spin $\delta = 0.019$, 0.067 and 0.182 (from bottom to top). Black line: Migdal-Eliashberg result. Lower panel: $U = 6t$ (above the critical value for Mott insulating behavior). Symbols: λ and δ as shown. Solid lines: Migdal-Eliashberg calculations, Eq. (8), with renormalized electron phonon couplings $\lambda_{\rm ren}$ and phonon frequencies $\omega_0^{\rm ren}$ as indicated.

still coincides with $\omega_0^{\rm ren}$. Thus, although a Migdal-Eliashberg analysis of self energies in high-T_c materials is problematic, the association of kinks in dispersions with phonon features [22] may be robust.

To summarize: we have introduced a method which enables simulations of impurity models with electron-phonon coupling at essentially the same computational cost as the corresponding models without phonons. We used the method to compute the phase diagram for the doping driven Mott transition in the Holstein-Hubbard model and the frequency dependence of the self energy. Previous work by one of us and by other groups [8, 14] had argued on the basis of Fermi liquid theory that the effect of phonons on correlated systems should be similar to that in uncorrelated systems, but with renormalized couplings. We found that this expectation is simply wrong at strong interactions in a half-filled model, but applies for large enough fillings and in the doped Mott insulating state as long as the quasi-particle energy is larger than the phonon frequency.

The approach presented here generalizes to other models which can be decoupled by Lang-Firsov transformations. In the Holstein-Hubbard model the interplay between superconductivity and strong correlations is an important open problem. Further generalizations are possible, for example to Jahn-Teller couplings in multiorbital models – although if pair-hopping terms are important one must perform a double-expansion in these and in the hybridization. Application of the method introduced here to models of manganites and to C_{60} (if the electronic spectrum is truncated to the 5 levels nearest to the chemical potential) seems entirely feasible.

The calculations have been performed on the Hreidar beowulf cluster at ETH Zürich, using the ALPS-library [23]. We thank M. Troyer for the generous allocation of computer time, K. Ziegler for helpful discussions, and NSF-DMR-040135 for support.

[1] A. Lanzara *et al.*, Nature **412**, 510 (2001).
[2] O. Gunnarsson, Rev. Mod. Phys. **69**, 575 (1997).
[3] M. Capone *et al.*, Science **296**, 2364 (2002).
[4] A. J. Millis, P. B. Littlewood and B. I. Shraiman, Phys. Rev. Lett. **74**, 5144 (1995).
[5] A. Yamasaki *et al.*, Phys. Rev. Lett. **96**, 166401 (2006).
[6] J. K. Freericks, and G. D. Mahan, Phys. Rev. B **54**, 9372 (1996).
[7] M. Tezuka, R. Arita, H. Aoki, Physica **359B**, 708 (2005).
[8] Ju H. Kim *et al.*, Phys. Rev. B **40**, 11378 (1989).
[9] M. Grilli *et al.*, Nuc. Phys. **B744**, 277 (2006).
[10] P. Benedetti and R. Zeyher, Phys. Rev. B **58**, 14320 (1998); J. P. Hague and N. d'Ambrumenil, cond-mat/0106355.
[11] J. Bonca, T. Katracnik, and S. A. Trugman, Phys. Rev. Lett. **84**, 3153 (2000).
[12] A. S. Mishchenko and N. Nagaosa Phys. Rev. Lett. **93**, 036402 (2004).
[13] A. Georges *et al.*, Rev. Mod. Phys. **68**, 13 (1996).
[14] A. Deppeler and A. J. Millis, Phys. Rev. B **65**, 224301 (2002); *ibid* 100301 (2002); cond-mat/0204617.
[15] W. Koller *et al.*, Europhys. Lett. **66**, 559 (2004); Phys. Rev. Lett. **95**, 256401 (2005).
[16] M. Capone *et al.*, Phys. Rev. Lett. **92** 106401 (2004).
[17] A. J. Millis, R. Mueller, and Boris I. Shraiman, Phys. Rev. B **54** 5389 (1996); S. Blawid, A. Deppeler, and A. J. Millis, Phys. Rev. B **67**, 165105 (2003).
[18] P. Werner *et al.*, Phys. Rev. Lett. **97**, 076405 (2006).
[19] P. Werner and A. J. Millis, Phys. Rev. B **74**, 155107 (2006).
[20] E. Gull *et al.*, cond-mat/0609438.
[21] I. G. Lang and Y. A. Firsov, Sov. Phys. JETP **16**, 1301 (1962).
[22] T. P. Devereaux *et al.*, Phys. Rev. Lett. **93**, 117004 (2004).
[23] M. Troyer *et al.*, Lecture Notes in Computer Science **1505**, 191 (1998); F. Alet *et al.*, J. Phys. Soc. Jpn. Suppl. **74**, 30 (2005); `http://alps.comp-phys.org/` .